Characterisation and deployment of an immobilised pH sensor spot towards surface ocean pH measurements

Jennifer S. Clarke, Eric P. Achterberg, Victoire Rérolle, Samer Abi Kaed Bey, Cedric F.A. Floquet, Matthew C. Mowlem

Analytica Chimica Acta 897 (2015) 69–80

Contents lists available at ScienceDirect

Analytica Chimica Acta

journal homepage: www.elsevier.com/locate/aca

Characterisation and deployment of an immobilised pH sensor spot towards surface ocean pH measurements

Jennifer S. Clarke [a, *], Eric P. Achterberg [a, b], Victoire M.C. Rérolle [d], Samer Abi Kaed Bey [c, e], Cedric F.A. Floquet [c], Matthew C. Mowlem [c]

[a] Ocean and Earth Sciences, National Oceanography Centre Southampton, University of Southampton, Southampton, SO14 3ZH, UK
[b] GEOMAR Helmholtz Centre for Ocean Research, 24148 Kiel, Germany
[c] National Oceanography Centre Southampton, Southampton, SO14 3ZH, UK
[d] Sorbonne Universités (UPMC, Univ Paris 06)-CNRS-IRD-MNHN, LOCEAN Laboratory, 4 place Jussieu, F-75005 Paris, France
[e] American University of Science & Technology, Alfred Naccache Avenue, P.O. Box 16-6452, Beirut, Lebanon

HIGHLIGHTS

- Immobilised pH sensor spot characterised over a pH range 7.8–8.2.
- Response time of 50 s at 25 °C.
- Temperature and Salinity dependence investigated.
- Deployed as an autonomous underway sensor.
- Achieved shipboard precision of 0.0074 pH in the Southern Ocean, over one month.

GRAPHICAL ABSTRACT

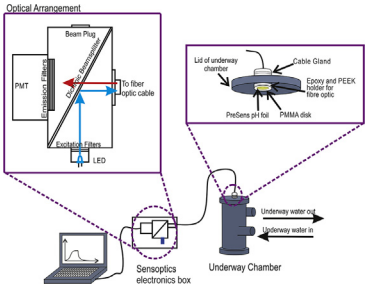

ARTICLE INFO

Article history:
Received 24 March 2015
Received in revised form
4 September 2015
Accepted 14 September 2015
Available online 25 September 2015

Keywords:
Seawater
pH sensor
Fluorescence
Optode
Ocean acidification

ABSTRACT

The oceans are a major sink for anthropogenic atmospheric carbon dioxide, and the uptake causes changes to the marine carbonate system and has wide ranging effects on flora and fauna. It is crucial to develop analytical systems that allow us to follow the increase in oceanic pCO_2 and corresponding reduction in pH. Miniaturised sensor systems using immobilised fluorescence indicator spots are attractive for this purpose because of their simple design and low power requirements. The technology is increasingly used for oceanic dissolved oxygen measurements.

We present a detailed method on the use of immobilised fluorescence indicator spots to determine pH in ocean waters across the pH range 7.6–8.2. We characterised temperature (−0.046 pH/°C from 5 to 25 °C) and salinity dependences (−0.01 pH/psu over 5–35), and performed a preliminary investigation into the influence of chlorophyll on the pH measurement. The apparent pK_a of the sensor spots was 6.93 at 20 °C. A drift of 0.00014 R (ca. 0.0004 pH, at 25 °C, salinity 35) was observed over a 3 day period in a laboratory based drift experiment. We achieved a precision of 0.0074 pH units, and observed a drift of 0.06 pH units during a test deployment of 5 week duration in the Southern Ocean as an underway surface ocean sensor, which was corrected for using certified reference materials. The temperature and salinity dependences were accounted for with the algorithm, $R = \left(0.00034 - 0.17 \cdot pH + 0.15 \cdot S^2 + 0.0067 \cdot T - 0.0084 \cdot S\right) \cdot 1.075$. This study provides a first step towards a pH optode system suitable for autonomous deployment. The use of a short duration low power illumination (LED current 0.2 mA, 5 μs illumination time) improved the lifetime and precision of the spot. Further improvements to the pH indicator spot operations include regular application of certified reference materials for drift correction and cross-calibration against a

* Corresponding author.
E-mail addresses: J.Clarke@noc.soton.ac.uk, jensclarke@gmail.com (J.S. Clarke).

http://dx.doi.org/10.1016/j.aca.2015.09.026

spectrophotometric pH system. Desirable future developments should involve novel fluorescence spots with improved response time and apparent pK_a values closer to the pH of surface ocean waters.

1. Introduction

During the period 2002–2011, global average atmospheric carbon dioxide (CO_2) concentrations increased by ~2.0 ppm per year; the highest rate of increase since monitoring began in the 1950s [1]. Atmospheric CO_2 concentrations are expected to continue to rise, with the ocean absorbing ca. 24% of the anthropogenically emitted CO_2 [2,3]. The current increase in atmospheric CO_2 is causing a surface ocean pH decrease of ~0.002 pH units per year [4–6], and a long-term pH decrease from a pre-industrial pH of 8.25 to today's pH of 8.1 [7]. The decrease in surface ocean pH has been observed at time series stations in both the North Atlantic and North Pacific Oceans [4]. Under the IPCC business-as-usual CO_2 emission scenario (IS92a) [8], Caldeira and Wicket have predicted further surface ocean decreases of up to 0.8 pH units by the year 2300 [9]. To monitor ocean pH and determine potential effects on ecosystems, *in situ* pH sensors are desirable. In this paper, we present an optode pH sensor based on fluorescent lifetime detection, for high resolution autonomous monitoring of surface ocean waters. The pH sensor was deployed as an autonomous shipboard system for surface water measurements in the Southern Ocean. The Southern Ocean is an important sink for CO_2 [10] due to low water temperatures and deep water formation, and is likely to suffer detrimental ecosystem effects as a result of ocean acidification [11]. The research cruise was a good platform to assess the suitability of the pH sensor for open ocean measurements, and marked a first step towards its application an *in situ* sensor. The research cruise was undertaken as part of the United Kingdom ocean acidification (UKOA) programme that investigated the effects of pCO_2 gradients in surface waters on biogeochemical processes, calcification and ecosystem functioning. Dissolved inorganic carbon (DIC) and total alkalinity (TA) measurements were undertaken, providing multiple opportunities for sensor validation.

1.1. pH sensors for oceanic waters

Optodes consist of a pH sensitive compound immobilised in a support matrix (termed sensor spot) and are typically placed at the end of a waveguide or fibre optic cable, which provides a channel for the excitation and emission light to travel [12]. pH optodes are not unique to environmental sensing; oxygen optodes are based on the same measurement principle, and have been deployed regularly for water column observations on CTD (conductivity, temperature & depth) rosette frames and Argo profiling floats, thereby demonstrating the great potential of the optode technology [13]. However, pH optodes have thus far only been deployed *in situ* in sediments yielding a precision of 0.0057 pH [14]. The motivation for characterisation of an optode pH sensor for deployment in open ocean waters using fluorescent lifetime detection was based on the perceived advantages of this approach over other technologies, recently reviewed in detail by Rérolle [15].

Other widely used techniques for pH measurements in seawater include potentiometric and spectrophotometric approaches [15]. Potentiometric pH systems are highly portable, with a measurement rate of 1 Hz [16], a precision of 0.003 pH units in the laboratory [17] and a shipboard accuracy of 0.01 pH [18]. However, prolonged measurements in high ionic strength solutions lead to inexact determination of the liquid junction and reference potentials of glass electrodes [16] resulting in measurement drift (0.05 pH $month^{-1}$) [18] and significant systematic errors [19]. Electrode drift can be tackled by regular recalibration using spectrophotometric measurements (monthly for individual electrode reference potential, and daily for electrode intercept potentials) [20] or calibration with pH buffers [21]. With seawater solution calibrations, pH electrodes have been successfully deployed on research cruises in estuarine and coastal environments with a precision of ca. 0.004 pH [22,23], and *in situ* in highly dynamic hydrothermal vent environments with a precision of ±0.06 pH [24].

Recently developed ion-selective field-effect transistors (ISFET) are a major advance in potentiometric pH measurements, and have been successfully tested in seawater [25] allowing analysis of up ca. 20 samples per minute [26] with a precision of 0.005 pH [27]. The sensors are known to drift between 0.03 and 0.05 pH upon initial deployment, though the exact magnitude of the drift will depend on the ISFET materials and packaging [28]. Long conditioning periods (1.5 months) prior to calibration can reduce this drift [25] and each sensor requires a full individual calibration prior to deployment [29].

Spectrophotometry is particularly well suited to seawater pH measurements and has been widely implemented *in situ* [15]; recent examples include the SAMI-pH instrument [30] and a high precision microfluidic system [31]. Spectrophotometric pH measurements have improved since their initial deployments in seawater, with precisions recorded as low as 0.0007 pH [32,33] and several systems achieving a precision of ca. 0.001 pH unit [34–38]. The use of wet chemical spectrophotometry requires indicator storage, as well as valves and pumps to propel sample and indicator solutions through the system. The reagents may have limited lifetimes (~1 year) and specific storage requirements (e.g. exclusion of UV), while bubbles and particles introduced in the fluidic system can interfere with the quality of the pH measurement [39]. Despite these potential issues, spectrophotometric SAMI-pH has been successfully deployed *in situ* for more than 2 years [40] and a microfluidic system with measurement frequencies of 0.5 Hz [35] has been demonstrated.

An ideal ocean pH sensor combines the limited calibration requirements of the spectrophotometric sensors with the simplicity and lack of mechanical components of the potentiometric sensors. Optodes are a newly emerging technology designed with both of these intended advantages.

1.2. Immobilised sensing spots

The pH sensing spots contain a pH-sensitive fluorescent dye (indicator) immobilised in a gas impermeable membrane attached to a support matrix. The practical measurement range is within ±1.5 pH units of the pK_a value of the indicator [41], where the pK_a is the isoelectric point at which the concentration of the acidic form of the indicator equals the basic form. The sensor spot's indicator pK_a can be altered with different immobilisation approaches, such as the type of membrane and support matrix used [12]. Immobilisation in more hydrophilic membranes such as cellulose results in smaller pK_a changes compared to more hydrophobic membranes such as polyurethane hydrogels [42]. Crosslinking within the

membrane may change the pore size, while charges in the membrane can affect both the sensitivity and pK_a [43]. The immobilisation technique also needs to be considered. Ionic associations between the membrane and the pH indicator 8-hydroxypyrene-1,3,6-trisulfonic acid (HPTS), for example, increases the apparent pK_a of HPTS, whereas the use of more covalent interactions lowers the apparent pK_a [44]. For applications in surface ocean samples, the pK_a of the immobilised indicator should be close to pH 7.7 to cover the oceanic pH range. The majority of immobilised pH indicators are based on fluorescein [45] and pyranine derivatives such as HPTS, due to their stability upon immobilisation, and a free pK_a ca. 7.3 which allows for measurements between pH 6 and 9 [44].

The pH of the sample solution determines the fluorescence emission of the pH indicator; the protonated and deprotonated forms of the indicator dye fluoresce at different wavelengths. Methods based on the measurements of fluorescence intensity alone have several inherent problems, such as sensitivity to light source fluctuations, background light and solution turbidity [46,47]. The additional immobilisation of a pH-insensitive fluorescent reference dye alongside the indicator dye allows measurement by dual lifetime referencing (DLR) or intensity ratiometric methods, thereby reducing the problems from intensity only measurements [46,48]. Intensity ratiometric methods utilise the intensity ratio between the indicator and reference dye emissions, requiring that the reference dye has similar optical properties to the indicator [41]. For DLR, the reference dye must be pH-insensitive, have similar or overlapping excitation and emission frequencies to the pH indicator dye, and a longer luminescent decay time.

There are two main DLR techniques: frequency-domain (*f*-DLR) and time-domain (t-DLR) [49]. The *f*-DLR technique continuously illuminates the spot with amplitude modulated light, and uses the phase-angle between the excitation and the dye fluorescence [50] to determine pH. The t-DLR technique takes a ratio of two "windows" of measurement [46]: one during the excitation of the spot with the light source and one during the fluorescence decay [48]. The t-DLR is a well-established methodology [46] which gives an instant visual response to pH changes. Both *f*-DLR and t-DLR techniques are not affected by light intensity fluctuations, optical alignment changes, and luminophore concentration [46]. In this study, we apply the t-DLR method to the sensing spots.

The pH sensor spots provide reproducible results [51] without the need for moving components, fragile electrodes or wet chemical reagents. The sensing spots are small (7 mm diameter) and require limited maintenance. Accuracy is improved by regular measurements of a certified reference material (CRM) to determine potential drift (see Section 2). The spots can be used directly with no sub-sampling of discrete solutions, and the technique has a comparable measurement time (5–200 s; see Table 1) to *in situ* spectrophotometric methods (ca. 60 s [32]–180 s [33]). Response times are diffusion controlled, and are proportional to the thickness of the membranes used (1–20 μm). Recent work with immobilised pH sensors in marine sediments has demonstrated a less favourable precision (from repeated measurements of CRMs) [52] compared with spectrophotometric measurements; average of 0.02 pH [53] and 0.001 pH [31], respectively, discussed further below.

Ambient light and excitation light exposure causes the indicator molecules to bleach, and thereby become less sensitive for pH measurements, eventually requiring replacement of the spot. If the reference dye and the pH indicator bleach at different rates then drift will be observed, affecting the accuracy of the pH measurements. This light sensitivity has limited the application of pH sensing spots to marine sediments (Table 1) [14,51,53,54]. Advances in oxygen optode technologies [13], and their use throughout the water column indicate the potential suitability of optodes for oceanic water pH measurements. In this work, we have characterised the pH sensor-spot technique for seawater application and present the first open ocean application. We first investigate the temperature and salinity dependences of the pH optode, then constrain the response time and provide an initial estimate for the longevity of the spot. We further discuss a test deployment in the Southern Ocean, and subsequently evaluate our system with respect to potential applications.

Table 1
Details of reported spot-based pH optodes where, DHFA = 2′, 7′-dihexyl-5(6)-N-octadecyl-carboxamidofluorescein, DHFAE = 2′, 7′-dihexyl-5(6)-N-octadecyl-carboxamido-fluorescein ethyl ester, DHPDS = Disodium 6, 8-dihydroxy-1, 3-pyrenedisulfonate, HPTS = 8-hydroxypyrene-1, 3,6-trisulfonic Acid, DSLR = digital single-lens reflex camera and CTAB = cetrimonium bromide. R = fluorescence ratio.

Reference	pH precision	Response times	Specifics	Range (pH)	Deployment & *Longevity*
Schröder & Klimant [53,55]	0.02	<200 s	DHFA and DHFAE with polyurethane hydrogel membrane and polyethylene terephthalate for support, and a charge-coupled device camera for analysis	7.2–9.2	4 days in marine sediments *1 week at 1 min measurement intervals*
Hakonen & Hulth [44,51]	0.0057	5 s	DHPDS with polyester spot and cellulose acetate membrane, analysis using a spectrofluorometer.	6–9	Marine sediments samples *160,000 measurements/ month*
Zhu, Aller & Fan [54]	~0.2 (precision in the ratio between 2 measured wavelengths)	<2 min	HPTS covalently linked onto a poly(vinyl alcohol) membrane backed with a polyester sheet and analysis using a DSLR camera	5.5–8.6	2 months in marine sediments and overlying water *Not Specified*
Wencel, MacCraith & McDonagh [56]	0.02	12 s	HPTS ion-paired with cetrimonium bromide (CTAB) in a sol–gel membrane, analysis using a spectrofluorometer with xenon lamp	5–8	None specified *1h illumination decreases R by 1%*
Larsen et al. [14]	0.02	60 s	HPTS and macrolex Yellow with polyurethane hydrogel membrane and polyester support, analysis using a DSLR	6–9	Marine sediments *>7200 measurements*
Current work	0.0074	50 s at 25 °C	PreSens spot using SensOptics electronics and a photomultiplier tube (PMT)	7–8.2 seawater	Surface seawater *>254 measurements over 3 days*

2. Materials & Methods

2.1. Additional instrumentation and reference materials for pH measurements

A glass electrode (ROSS Ultra® combination pH electrode with epoxy body) with a benchtop pH meter (Thermo Scientific Orion 3*) was used for reference potentiometric pH determinations (precision of 0.01 pH). The glass pH electrode used internal temperature compensation derived from the Nernst equation [57]. National Institute of Standards and Technology (NIST) pH buffers (pH 4, 6, 7, 10; Sigma–Aldrich) and Certified Reference Material (CRM) tris (2-Amino-2-hydroxymethyl-propane-1,3-diol) buffer in artificial seawater (Batch 10, pH_{tot} 8.0924, salinity 35, 25 °C) from Prof. A. Dickson at Scripps Institute of Oceanography (USA) were used to calibrate the pH glass electrode for low and high salinity measurements, respectively. A lab-on-a-chip microfluidic spectrophotometric pH sensor with thymol blue indicator (indicator concentration of 2 mmol L^{-1}, precision of 0.001 pH), was used as a reference for the higher salinity pH analyses. The thymol blue extinction coefficients were determined in the laboratory (e1 = 0.0072, e2 = 2.3, e3 = 0.18) and the indicator's dissociation constant (pK_2 = 8.5293) was taken from Zhang and Byrne [58]. The reader is referred to Rérolle et al. (2013) for further detail on the instrument and analytical approach [15]. The temperature of the samples during laboratory measurements was controlled using a water bath (Fluke Hart Scientific 7012, ±0.1 °C). All pH values reported in this paper are on the total pH scale. Temperature of the solutions was checked prior to measurement with a DT-612 dual input K-type thermometer (ATP, ±0.1 °C).

2.2. pH buffer solutions

The pH optode sensor was characterised at different pH values, salinities and temperatures. Non-equimolar tris pH buffers were prepared in artificial seawater according to Pratt [59]. For this purpose 1 mol kg^{-1} magnesium chloride ($MgCl_2$) and calcium chloride ($CaCl_2$) solutions were calibrated using gravimetric Mohr titrations [60]. Hydrochloric acid (HCl, 1 mol kg^{-1}) was calibrated using a gravimetric borax titration [61]. Other salts (sodium chloride, sodium sulfate, tris, and potassium chloride) were dried at 110 °C for 1 h prior to weighing. Deionised water (MilliQ, Millipore, >18.2 MΩ cm^{-1}) was used to prepare and dilute all solutions. All chemicals used in the preparation of artificial seawater were of analytical grade from Sigma–Aldrich. Stock buffer solutions (50 ml) over a pH range of 7.0–8.3 were made by combining tris salt (0.08 mol $kg(H_2O)^{-1}$), hydrochloric acid and small amounts of sodium chloride with deionised water. The pH was altered by adjusting the ratio of acidic to basic tris (HCl to tris salt), keeping the concentration of tris constant (0.08 mol $kg(H_2O)^{-1}$) and varying the HCl concentration. The small amount of sodium chloride in the stock buffer was varied to account for the changing ionic strength contribution from the HCl. These 50 ml buffer solutions were then made up to the desired salinity with 25 ml of stock artificial seawater, in turn made up from sodium chloride, sodium sulfate, magnesium chloride, calcium chloride and potassium chloride.

To study the temperature dependence of the sensor over the temperature range of 5–25 °C, an array of 8 tris buffers with pH ranging from 7 to 8.3 were prepared at a fixed ionic strength of 0.7 M. The pK_a of tris has a strong temperature dependence (0.03 pH °C^{-1}) [62]. The pH range of the buffers was therefore selected to obtain the desired pH range of 7.6–8.3 over the varying temperature range of the experiment.

To study the salinity dependence of the optodes, an array of 7 tris buffers with pH values ranging from 7.8 to 8.2 with salinities of 5, 25 and 35 were prepared, following the method of Pratt [59]. 200 mL batches of lower salinity (5 and 25) artificial stock seawater without HCl and tris were prepared by dilution of concentrated artificial seawater (142 ml and 16 ml of the salinity 35 seawater made up to 200 ml in deionised water). The stock buffer solutions were the same as salinity 35 seawater, regardless of the final salinity desired for the buffer solution. The 25 ml of stock seawater was added to the buffer solutions to make up the analysis solutions. The ratio between the salts was kept constant, and only the ratio of salt to water was varied to provide the different salinities.

2.3. pH optode hardware

A 5 mm diameter blue light emitting diode (LED, 470 nm, Farnell) with excitation filters (SemRock single bandpass filter 475 nm and SemRock short pass edge filter 532 nm) was used at low intensity (0.2 mA, 0.72 mWatts) to excite the reference and indicator dyes within the immobilised sensor spot for periods of 5 μs, thus minimizing bleaching. The blue excitation light was reflected off a dichroic beam splitter (SemRock single edge BrightLine, 560 nm) through a fibre optic cable (600 μm diameter multimode optical fibres, Thorlabs, 3.8 mm diameter tubing, 1 m length) to the pH sensitive spot. The excited fluorophores subsequently emitted a fluorescence signal (630 nm) that decayed over time. The red light passed through the dichroic beam splitter, and three emission filters (SemRock single bandpass filter 609 nm, SemRock short pass edge filter 785 nm and SemRock long-pass edge filter 568 nm) before entering the detector. Due to the low level of light involved, the detector was a photon multiplier tube (PMT; Hamamatsu). The spot interrogation system used a field-programmable gate array (Xilinx Spartan-3 XC3S400-5PQ208C FPGA) to control the PMT and LED.

Custom-made electronics (Sensoptics Ltd[1], SGS 42000) were used with dedicated software (Sensoptics Photon Counter V1.2) to record the fluorescence decay curve. A diagram of the hardware setup is shown in Fig. 1.

The sensor spot (PreSens, non-invasive pH spot, SP-HP5-D7) was glued to a clear poly (methyl methacrylate) (PMMA) disc using silicone rubber glue (RS Silicone rubber glue, 692-542). Tests showed a negligible autofluorescence effect from the PMMA and glue. The set-up was left to dry for 2–3 days in the dark before being fastened using epoxy glue (Intertronic, OPT500149) to a polyether ether ketone (PEEK) head attached to the fibre optic cable (600 μm diameter multimode optical fibre, Thorlabs, 3.8 mm diameter tubing, 1 m length). The fibre optic cable was wrapped using a rubber coating to minimise light loss and ambient light penetration, and connected directly to the PMT at the distal end of the fibre. The PEEK head with sensor attached was stored in artificial seawater (at the specific salinity under investigation) to soak for at least half a day prior to measurements, as recommended by Stahl and co-workers [55]. Preconditioning allowed the sensor to adjust to the salinity/ionic strength of the measurement solution, and prevented leaching of indicator and reference dyes during measurements, which (if it occurred during the measurement) would result in signal reduction [55]. This also allows any chemicals from the glues and epoxy to leach prior to characterisation and deployment. To minimise photo bleaching of the indicators by ambient light, the sensor was covered with thick, dark, 'blackout' material and the laboratory work was performed in a dark room. Field measurements were undertaken with the pH optode positioned in a custom-made dark chamber.

[1] Sensoptics is now a wholly owned subsidiary of Optasense (A QinetiQ company) http://www.optasense.com.

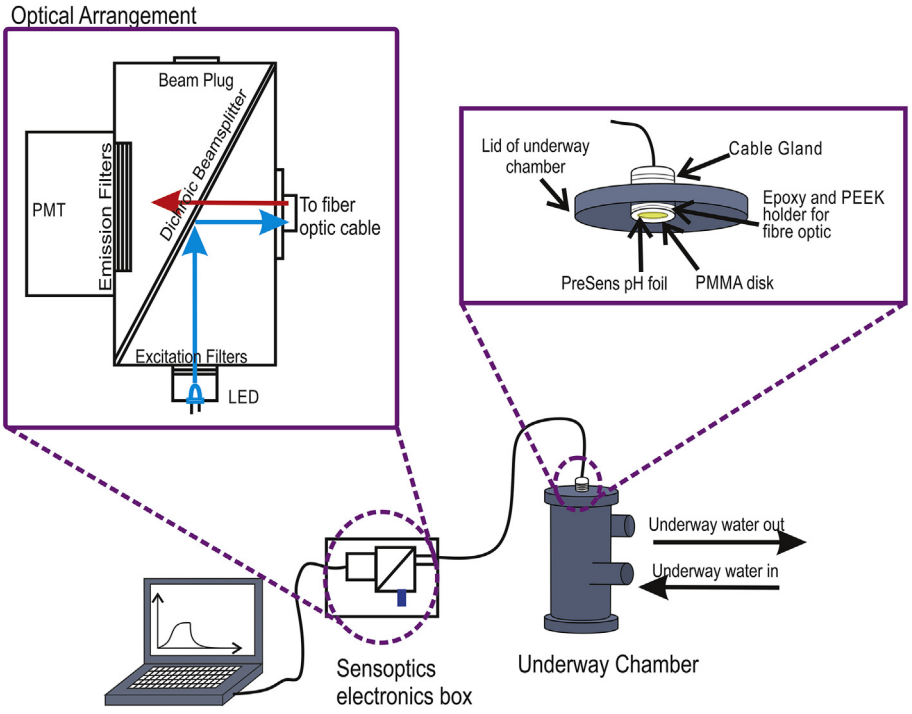

Fig. 1. Schematic of the sensor for use as a shipboard autonomous underway system.

2.4. Analytical protocol for pH measurements

pH indicators are weak acids and bases and hence have a capacity to respond to changes in solution pH through proton exchange. In high pH solutions, the indicator donates protons and takes its basic form, and in low pH solutions, the indicator accepts protons and takes its acidic form. The different forms of the indicator fluoresce differently allowing the pH of the solution to be determined.

To produce a single pH data point, the light source (blue light emitting diode (LED)) is pulsed using a square wave mode, with the LED on for 5 μs (t_{ex}) and the LED off for 20.5 μs (t_{em}). The LED light excites the pH indicator causing the dye molecules to fluoresce. When the LED is off, the fluorescence gradually decays. The fluorescence decay is recorded in 100 ns bins for 20.5 μs. This is repeated 19,608 times, and averaged to give an average fluorescent decay profile every 0.5 s. Higher precision and an improved signal to noise ratio are achieved by recording each sample for 200 s and integration of the profiles at 10 s intervals.

With the LED on, the emission (t_{ex}) is a combination of fluorescence from the pH sensitive (A_{pH}) and reference fluorophores ($A_{ref\text{-}ex}$), shown in Fig. 2 with blue and red lines respectively. The variation in fluorescence recorded in the first 5 μs is dominated by the indicator dye, and is related to the pH of the solution. We assumed that the integration of the fluorescence intensity when the LED is off, (t_{em}) is entirely derived from the decay of the pH-insensitive reference dye emission ($A_{ref\text{-}em}$) due to the shorter decay lifetime of the pH sensitive fluorophore. The intensity of the first 5 μs of the profile (excitation period where the LED is on) is summed for each profile and referred to as t_{ex}. The intensity of the last 20.5 μs (emission period when the LED is off) is summed and referred to as t_{em}. The ratio of t_{ex} over t_{em} (R, Equation (1)) is converted to pH using Equation (2) which includes terms (a–g) for temperature and salinity dependence (specified in Section 3.6).

$$R = \frac{t_{ex}}{t_{em}} = \frac{A_{pH} + A_{ref-ex}}{A_{ref-em}} \quad (1)$$

$$R = \left(a + (b \cdot pH) + \left(c \cdot S^2\right) + (e \cdot T) - (f \cdot S)\right) \cdot g \quad (2)$$

The apparent pK_a (here onwards denoted as pK_a') of the indicator, is the pK_a where concentrations are used without the relevant activity coefficients to correct for the non-ideality of real solutions. The apparent pK_a therefore displays not only temperature dependence, but also dependence on factors that affect the activity coefficients, such as ionic strength [63]. Without detailed

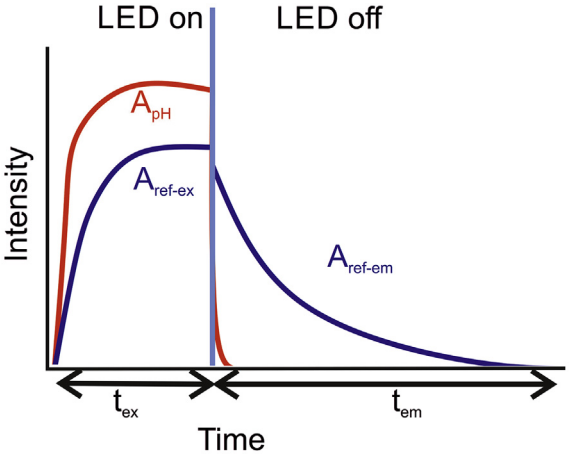

Fig. 2. Fluorescence intensity change with time as a result of switching on and off LED light source. Signal is used to obtain the time domain-Dual Lifetime Referencing ratio (R) from the integration of the emission intensity over two windows: t_{ex}/t_{em}. The LED on emission (t_{ex}) can be broken down into the emission of the excited pH sensitive dye (A_{pH}, red line) and the excited pH insensitive dye (A_{ref-ex}, purple line). The LED off emission (t_{em}) is assumed to consist solely of the pH insensitive dye (A_{ref-em}). The reference fluorescence (A_{ref-ex} and A_{ref-em}) has a long lifetime and is independent of pH, while the fluorescent intensity of the pH sensitive dye varies with pH and has a short lifetime (A_{pH}). Curve and equation adapted from Schröder et al. (2005) [53]. (For interpretation of the references to color in this figure legend, the reader is referred to the web version of this article.)

knowledge of the indicator, the relevant activity coefficients could not be used when determining the pK_a and therefore pK_a' was used in this study.

To determine the pK_a' of the pH indicator, and therefore the measurement range of the sensor, the optode was immersed in tris/2-aminopyridine buffer solutions with a salinity of 5, prepared according to Section 2.1, with pH values ranging from pH 9 to 5. The pK_a' was determined using Equation (3) [64] and 4 [65], according to the method of Salgado and Vargas-Hernández [66] (see Fig. 3). The term A in equation and Fig. 3 is the fluorescence intensity caused by a specific solution pH, A_{Basic} is the maximum fluorescence output at pH 9, corresponding to the conjugate base form of the indicator (A^-), and A_{Acidic} is the minimum fluorescence output at pH 5, corresponding to the acidic form (HA). The total indicator concentration at basic pH and maximum fluorescence is proportional to $(A_{Basic} - A_{Acidic})$. The concentration of the basic form of the indicator $[A^-]$ at any pH is proportional to $(A - A_{Acidic})$. The concentration of acid form [HA] at any pH is proportional to $(A_{Basic} - A_{Acidic}) - (A - A_{Acidic}) = (A_{Basic} - A)$. The ratio of the abundance of acidic and basic forms of the indicator is equal to one when $pK_a' = pH$ as indicated by Equation (4) (Henderson–Hasselbalch equation). The pK_a' of the indicator can be obtained through linear regression of $-\log (A_{Basic} - A)/(A - A_{Acidic})$ against the pH of each solution, with the y-intercept divided by the gradient yielding pK_a'.

$$[HA]\Big/\left[A^-\right] = (A_{Basic} - A)/(A - A_{Acidic}) \quad (3)$$

$$pH = pK_a + \log\left(\left[A^-\right]\Big/[HA]\right) \quad (4)$$

To investigate the effects of temperature variations on pH measurement, the set of tris pH buffers (as in Section 2.2) at salinity 35 was equilibrated in the water bath for a period of 15 min followed by pH measurements using both the reference glass electrode (as detailed in Section 2.1) and the sensing spot. The buffers remained in the water bath (as above, Fluke Hart Scientific 7012) during the measurements. The temperatures used for the calibration procedure were 5, 10, 15 and 25 °C. Temperatures of the samples were verified with a DT-612 thermometer (as above ATP, ±0.1 °C). Each sample was measured three times and the results averaged (see Fig. 4). If the pH as recorded by the reference glass electrode over the three repeats deviated more than 0.003 pH units, the samples were not averaged and the samples outside the deviation limit (0.003 pH) were treated as separate samples. This deviation limit (±0.003 pH) is equivalent to the temperature induced pH change in the tris buffer from the uncertainty in the thermometer measurement (±0.1 °C).

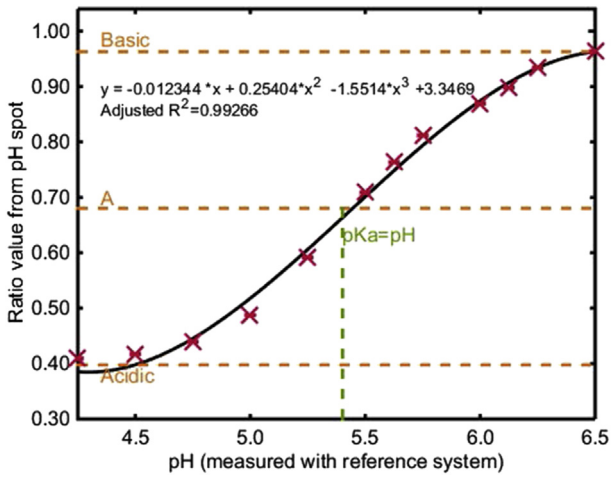

Fig. 3. Sigmoidal shaped fluorescence ratio response from measurements of salinity 5 buffer (tris and 2-aminopyridine) solutions. pH measured with a glass pH electrode. The horizontal orange dotted lines relate to the values in Equation (2), and the vertical dotted green line is the equivalence point where $pH = pK_a'$. (For interpretation of the references to color in this figure legend, the reader is referred to the web version of this article.)

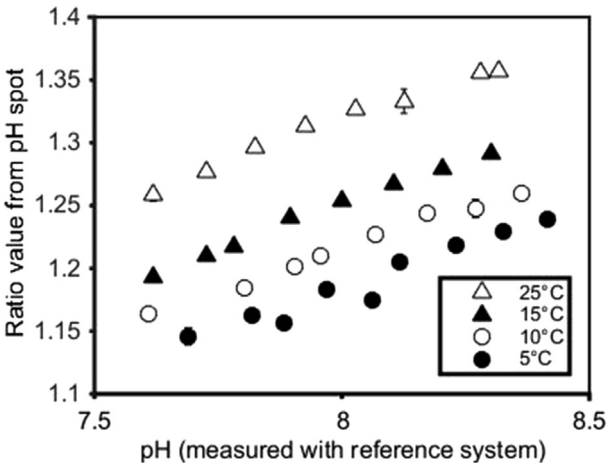

Fig. 4. Response of the pH spot to temperature variations. Samples of tris buffered artificial seawater were analysed at temperatures between 5 °C and 25 °C. Reference pH was determined using a glass pH electrode calibrated with tris buffered CRM [79]. Where error bars cannot be seen, they are smaller than the size of the marker.

To investigate the effects of salinity on the pH spot, the set of buffer solutions prepared at different salinities (as in Section 2.2) were equilibrated in the water bath at 25 °C for a period of 15 min followed by pH measurements using both the reference glass electrode (as detailed in Section 2.1) and the sensing spot. Each sample was measured three times and averaged (see Fig. 5).

Samples of salinity 35 were also measured with the spectrophotometric pH system (Section 2.1). The temperature was maintained at 25 °C, with the samples incubated for 15 min prior to measurement.

To study the response time of the sensor, repeat alternating measurements were made of two tris buffered seawater solutions (salinity 35) with pH values of 7.2 and 8.5 at 25 °C. These pH values are at the limits of the intended measurement range. The measurements were recorded for a period of 200 s before the optode was rinsed with deionised water and transferred into the next solution; this process was repeated 25 times. The time required for the optode to reach 97% of its final stable R (t_{97}) from first being placed in the solution is quoted as the response time, similar to the method of Tengberg and co-workers [67]. Precision of the pH optode measurements was determined from analysis of the pH CRM tris buffer and a CRM for Total Alkalinity (TA)/Dissolved Inorganic Carbon (DIC) (Prof. A. Dickson, Scripps) at 25 °C [68].

In order to determine the lifetime of the spot, a new spot (glued to PMMA disc and left to precondition for 2 days prior to use) was attached to the optode. It was then illuminated continuously for one hour with the LED at 0.72 mWatt (0.2 mA, normal excitation level). A 200 s measurement was taken before and after the continuous illumination to assess the change in the response. This was performed in a water bath at 25 °C, in artificial (salinity 35) seawater. The sample was not changed between measurements and continuous illumination. The continuous excitation of the spot for one hour amounted to 720×10^6 LED cycles. In case of a typical pH measurement, the spot is only excited for one fifth of the total

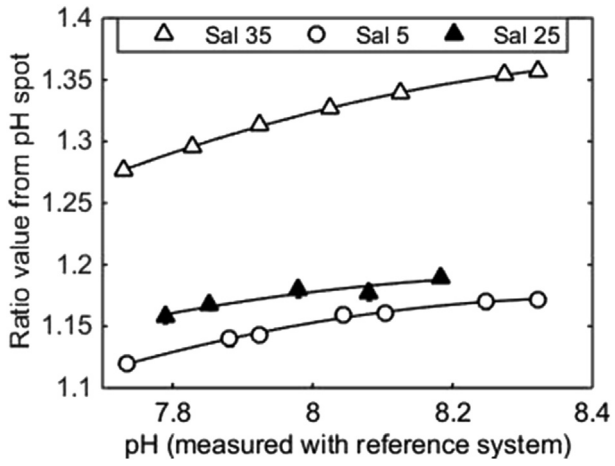

Fig. 5. Response of the sensor spot to varying salinity of the solution from 5 to 35 psu over a range of pH values measured with the reference electrode. Reference pH was determined using a glass electrode calibrated with tris buffered CRM for high salinity samples and NIST buffer solutions for very low salinity samples. Where error bars cannot be seen, they are smaller than the size of the marker.

measurement and the hour-long continuous illumination was hence equivalent to 7200 decay profiles, 367 measurements of 50 s (response time) or 92 measurements assuming a 200 s measurement time.

An additional test was performed with the optode recording 200 s measurements with the short illuminations, as opposed to the continuous illumination. The spot was set to run for 3 days in buffered artificial seawater in a sealed container to maintain constant pH at 8.1. The spot response was recorded for 200 s every 15 min, for 254 measurements.

An investigation into the effect of chlorophyll-*a* on measured R was undertaken using *Emiliania huxleyi* (obtained from the Roscoff culture collection (RCC), strain number RCC1228). The *E. huxleyi* was cultured at 16 °C, under 100 μE light and diluted to specific chlorophyll-*a* concentrations (0.13, 0.68, 1.02, 2.05, 3.42 and 6.84 μg L^{-1}) with salinity 35 seawater. The pH of the seawater was measured with the reference glass electrode prior to measurement with the optode. Measurement of the solutions was performed in the dark, and at 25 °C in a water bath for both the electrode and the optode. The pH was not constant during the characterisation and the effect on R was removed by normalising the ratio (R) to a pH of 8.09 using the following equation

$$R_n = \frac{R \cdot 8.09}{pH_{soln}}$$

Where pH_{soln} is the pH of the solutions determined by electrode, and R is the measured ratio and R_n is the normalised ratio.

2.5. Cruise deployment details

The sensor was deployed aboard the R.R.S. *James Clark Ross* in the Southern Ocean in the period January–February 2013 (cruise JR274) as part of the UKOA Programme (http://www.surfaceoa.org.uk). Over the period January 22 to 26, 2013, pH measurements were undertaken along a diagonal transect north of South Georgia (54–49 °S, 38–40 °W). The pH sensor was placed in the ship's main laboratory connected to the continuous underway seawater supply, which had an intake at ca. 7 m depth, and measurements were conducted without filtration. Temperature and salinity measurements in the underway seawater supply were conducted using a thermosalinograph (SeaBird Electronics, Inc, SBE 45 thermosalinograph fluorometer) fitted in the preparation laboratory. Samples for DIC and TA were collected at hourly intervals along this transect. Measurements of pH_{tot} from the DIC/TA CRMs were undertaken at the halfway of each spot deployment on the cruise; two spots were used across the cruise. The spot was changed on 23/01/13.

pH was calculated from certified values of DIC and TA using CO_2SYS [69] (Matlab v2.1) with carbon dissociation constants from Roy (1993) [70], sulphate dissociation constants from Dickson (1990) [71] and borate dissociation constants from Lee (2010) [72]. The calculated pH from the DIC and TA CRM measurements was compared to the sensor-measured pH and any drift from the certified value was corrected using the ratio between the measured and the calculated value. This calculation has an estimated error of ±0.0062, which is comparable to the current precision of the pH optode.

3. Results and discussion

3.1. pH sensor spot characterisation

To determine the pK_a' of the pH indicator, the optode was immersed in buffer solutions ranging from pH 9 to pH 5. This produced a sigmoidal-shaped fluorescent ratio (R) response (Fig. 3) from the varying fluorescence as the immobilised indicator transitioned from the basic form to the acidic form. The signal flattened at the acidic and basic ends of the sigmoid due to the fulfilment of the proton donation and acceptance capacity of the indicator molecules.

The value of R increased with increasing pH, indicating that the basic form of the indicator fluoresced more intensely compared with the acidic form. The most sensitive region for pH observations is where there is the highest change in R per change in pH. This occurs in middle of the sigmoidal shaped fit and demonstrates the viability of the sensor for seawater measurements (average surface ocean pH range ~7.9 to 8.2) [7]. A sigmoidal shaped response upon pH variations has also been reported for other pH optode systems with immobilised indicators [49,53,65,73,74].

The obtained pK_a' value was 6.93 at 20 °C, as determined using the approach detailed in Section 2.4, and denoted by the green dotted line in Fig. 3. Immobilisation of the fluorescent compound in the sensor spot caused the pK_a' to be lower than pK_a' of the free-form of HPTS (7.3) [74], and similar to the immobilised values reported by Hakonen [44]. This pK_a' is lower than the pH of seawater, but the measurement range is considered to be between ±1.5 pH units of pK_a', and hence covers the typical surface ocean pH range. Nevertheless, precision and accuracy may deteriorate at the edges of this range, i.e. near pH ca. 5.4 and 8.4. Temperature and salinity effects on the pK_a' of free (non-immobilised) pH indicator have been evaluated by other workers [75,76] and pH calibrations with immobilised sensors have been reported, although none specifically for open ocean use. This study's novel application of the optode and immobilised sensor requires characterisation at temperatures and salinities relevant to these environments.

3.2. Temperature dependence

The temperature of artificial seawater with tris pH buffer was varied between 5 °C and 25 °C in order to quantify the temperature effect on the fluorescent indicator response. An increase in R was observed when comparing solutions with the same pH analysed at increasing temperatures (Fig. 4). The overall temperature dependence was determined from the gradient of the linear regression, −0.046 pH $°C^{-1}$ over the temperature range of 5–25 °C.

This increase in R with temperature can be attributed to a decreased quantum yield at higher temperatures for both

fluorophores from increased internal and external conversions of the fluorescence energy in addition to the temperature influence on the pK_a' of the indicator [53]. The decreased quantum yield has a minor effect on the pH sensitive fluorophore due to the short decay time but due to the longer lifetime of the pH insensitive dye, a larger effect is seen when integrating the t_{ex} time window.

The observed temperature dependence of the pH spot is similar to that reported for an immobilised sensor spot by Schroeder et al. [53], but smaller than reported by Kirkbright et al. [77]. The temperature dependence requires the accurate recording of temperature and a correction of the final pH readings. Hakonen et al. [78] calibrated at two temperatures 25 °C and 15 °C, and extrapolated with a linear correlation to extend the system for use at lower temperatures, and found an error in pH of 0.01 pH units as a result of sharp temperature gradients. Schröder found pH errors of ca. 0.03 pH $°C^{-1}$, and did not correct for temperature variations smaller than 5 °C [53]. An alternative approach to avoid the complications of temperature corrections is to analyse pH in samples at a constant temperature [14,54,56]. With the ultimate aim to deploy our pH optodes *in situ*, the latter two approaches (measure at a constant temperature and apply no correction for deviations less than 5 °C) were deemed unsuitable. The temperature was included in the algorithm to convert R to *in situ* pH, with measurements over a wider range of temperatures compared to Hakonen et al. to better characterise the dependence, with the ultimate aim to correct for temperature-induced variations (Section 3.6).

3.3. Salinity dependence

Solutions of artificial seawater (S = 35) with tris pH buffer were diluted to salinities (5 and 25, see Section 2.2) and analysed at a constant temperature of 25 °C (Fig. 5). There was a significant difference between the R values at salinity 5 and both salinities 25 and 35 (student t-test $t = -2.765$ $n = 11$, *two-tailed* $p = 0.0184$ and $t = 12.875$, $n = 12$, *two-tailed* $p = 2.2 \times 10^{-8}$ respectively). The value of R increased with salinity with an overall dependence of −0.01 pH psu^{-1}, similar to the dependence reported by Schroeder et al. [53] and pH-salinity error of Hakonen et al. [78], 0.008 pH.

The increase in R with salinity is due to changes to the indicator pK_a' caused by surface–solution interactions between the spot and the surrounding buffer solution [79]. Theoretical considerations (Debye-Hückel) indicate that an ionic strength increase is accompanied by an apparent pK_a' decrease [74,75], and consequently for a constant pH there is an increasing concentration of the conjugate base form of the indicator. This causes an increase in R with salinity (Fig. 5). The lack of a significant difference between the lower salinity solutions (5 and 25), as shown in Fig. 5, indicates the presence of a secondary process. The ionic strength within the microenvironment of the spot is not just a consequence of the ionic strength of the external solution; charged molecules in the membrane and surrounding the indicator dye, will affect the pK_a' and thereby influence R. The pH at the surface of the optode (pH_{surf}) will be different to that of the bulk sample solution (pH_{bulk}), and is controlled by the surface potential (ψ) which is determined by the ionic species present at the interface between the optode surface and the bulk solution [79]. The charges in the membrane allow the surface potential to be unaffected by variations in the ionic strength of the sample solutions. This process thereby stabilises the observed pH_{surf}. However, at full seawater salinity (ca. 35), the sample ionic strength is greater than the apparent ionic strength at the surface. Therefore, the bulk ionic strength will influence the surface potential and causes the apparent indicator pK_a' to decrease and the R to shift to higher values [79].

Typical seawater salinities (35) cause a much larger change to R compared to brackish and estuarine salinities (e.g. 5–25). This indicates that the foil could be used without salinity correction in low salinity environments. Schröder [53] did not compensate for the salinity effects on the optode response as the changes observed were within the desired accuracy (0.02 pH units), while Hakonen et al. corrected for salinity deviations using log linear transformations. In order to obtain high quality surface ocean pH measurements for monitoring the changes to the oceanic carbonate system, the shift in R as a result of salinity/high ionic strength is included in the pH determinations (Section 3.6).

3.4. Chlorophyll influence

Fluorescent compounds present in seawater can potentially influence the sensor response by increasing the fluorescence counts in the t_{em} portion of the fluorescence decay curve. An investigation into chlorophyll-*a* interference was undertaken, involving pH analyses of solutions with increasing concentrations of chlorophyll-*a* from the coccolithophore, *Emiliania huxleyi*. The pH of the solutions was not controlled and normalisation was performed (see Section 2) to determine if there was an influence from the increasing chlorophyll. A decrease in R_n (up to 0.15 units, ca. 0.9 pH units) was observed at enhanced chlorophyll concentrations (between 2.05 μg L^{-1} and 6.5 μg L^{-1}). These concentrations are significantly higher than generally observed in the open ocean (ca. 0.1–1 μg L^{-1} www.earthobservatory.nasa.gov), but may be encountered in coastal waters. At lower chlorophyll concentrations (0–1 μg L^{-1}), the response showed a smaller increase in R_n (up to 0.05 units, ca. 0.3 pH units). The complex sensor response to chlorophyll fluorescence did not allow this to be included in a dependency algorithm (Equation (5)). Elimination of chlorophyll fluorescence was therefore deemed more appropriate. This could be undertaken by manufacturing a blackout layer on the surface of the optode, although this would increase the response time of the sensor, or by removal of phytoplankton cells through on-line filtration of seawater prior to analysis. Obviously, in waters below the sun-lit layer in the ocean, where there are no phytoplankton, this chlorophyll interference is not relevant.

3.5. Multi-linear regression for fluorescent signal conversion to pH

In order to convert the fluorescent signals obtained by the optode sensor to pH, a stepwise multi-linear regression was performed on data from the temperature and salinity investigations (n = 120). The regression yielded Equation (2), where T is temperature in °C and S is salinity, and R is the ratio as determined from the optode output with the coefficients specified below.

$$R = \left(0.00034 - 0.17 \cdot pH + 0.15 \cdot S^2 + 0.0067 \cdot T - 0.0084 \cdot S\right) \cdot 1.075 \quad (5)$$

The equation was derived for the pH range 7.6–8.3, a temperature range of 5–25 °C, and a salinity range of 5–35. It has an adjusted r^2 of 0.973 (n = 120), a standard error of pH is 0.005. The temperature and salinity data were obtained using a single spot. Differences between spots may occur during manufacturing process, which might create an offset when used with the above equation, but should not affect the temperature and salinity dependence determined here. To account for these offsets, CRM measurements should be used for calibration. As the chemistry of the commercial optode spots is assumed stable and repeatable, the temperature and salinity dependence calibration need only be performed for one spot (as in this study) and may then be applied to others.

A future re-calibration using a spectrophotometric system, would allow for improved accuracy in the characterisation of the

temperature and salinity dependence due to the greater precision of the spectrophotometric system compared with the potentiometric pH measurements. This approach will be similar to the use of a correction coefficient by Yang et al. [80], who applied this to broadband spectrometer measurements, thereby relating the data back to a narrowband calibration. This is postulated to improve the accuracy and precision of the sensor spot.

3.6. Metrology

Results from the response time experiment are presented Fig. 6. The upper line of measurements represents pH 8.5 (ratio ~1.13) and the lower line represents pH 7.2 (ratio ~0.73). The points in between represent the equilibration of the spot in the solution. The time required for the optode to reach 97% of its final stable R (t_{97}) was 50 s. This is comparable to results from similar sensors in marine sediments (Table 1 [14,51,54]; 5–200 s). The standard deviation of the ratio from the mean pH for each solution had an average value of 0.003 (n = 18), equivalent to 0.03 pH units (Fig. 6).

Comparison between measurements of salinity 35 tris buffers at 25 °C with the spectrophotometric system and the optode before temperature and salinity correction showed a good agreement (Fig. 7), with no statistically significant difference (student pairwise t-test, t = 0.737, df = 14, *two-tailed p*-value 0.473). The optode sensor algorithm (Equation (5)) yielded pH values that were 0.103 ± 0.03 pH units higher in the range 7.5–8.3 compared to the spectrophotometric sensor. A final calibration step of involving a CRM is consequently still required for the optode spot prior to use.

An experiment with continuous illumination of the spot was undertaken to give an indication of the number of measurements a single spot could make before bleaching of the indicator dye significantly affects the quality of the determination of R. A change in the ratio of <1% was observed from measurements before and after the continuous illumination for 1 h, similar to what is reported by other workers [14]. This indicates that the foil is stable for a minimum of 92 continuous measurements of 200 s. These estimates are the lowest limits of the lifetime of this spot due to the constant illumination, which is not the normal use of the foil.

The sensor drift was evaluated over three days with consecutive

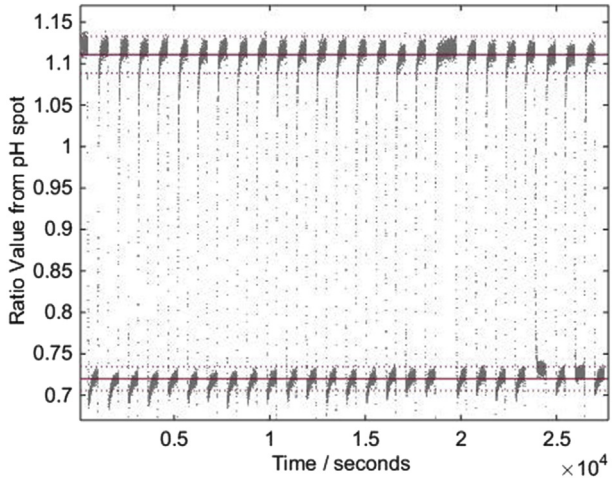

Fig. 6. Results of repeatability experiment. The sensor was repeatedly switched between seawater solutions of pH 7.2 and 8.5. The upper line of measurements represents pH 8.5 (ratio ~ 1.13) and the lower line (ratio ~ 0.73) pH 7.2. The points in between are the equilibration of the spot in the solution. The straight red line shows the ratio mean for the two pH solutions, and the dotted lines show 98%of the mean (final value). (For interpretation of the references to color in this figure legend, the reader is referred to the web version of this article.)

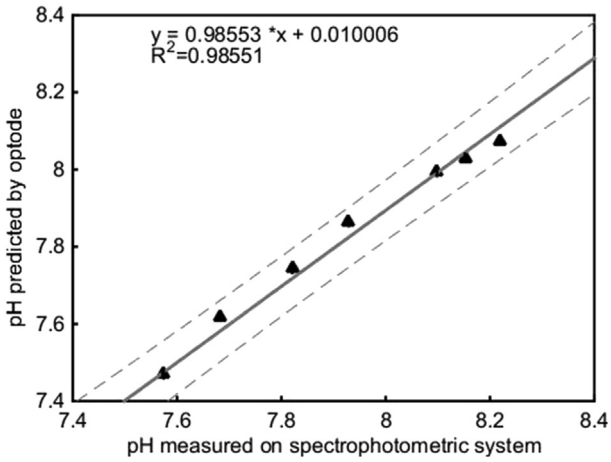

Fig. 7. Comparison of the pH determined by the pH optode sensor against the measured spectrophotometric sensor values. Error bars are shown for both x and y measurements, based on the standard deviation of the repeat measurements (n = 3) – x and y error bars are obscured by the size of the marker. The dotted lines represent the 95% confidence limits. Measurements of salinity 35 tris buffer in artificial seawater were undertaken in a water bath at 25 °C, for both sensors.

200 s measurements (Fig. 8). The standard deviation (σ) across the 254 measurements over the three days was 0.0013 R (ca. 0.016 pH, at 25 °C, salinity 35); with a small downward drift of 0.000014 R (ca. 0.0004 pH, at 25 °C, salinity 35). This drift was smaller than the standard deviation across all the measurements. However, the measurements showed smaller variability in R over a 3 day period (σ = 0.0013) with the shorter illumination cycles compared to the variability in R after the continuous illumination experiment (1 h, σ = 0.01). This indicates that the shorter illumination times are advantageous in prolonging sensor spot use. Furthermore, according to other workers, the calibration of sensor spots is retained during dark storage for periods of months [54,56].

3.7. Cruise data

Over 3000 data points were collected on a research cruise in the Southern Ocean, involving the use of two spots (~1500 data points each). The first spot was replaced during the cruise due to concerns of light exposure and consequent photo bleaching during

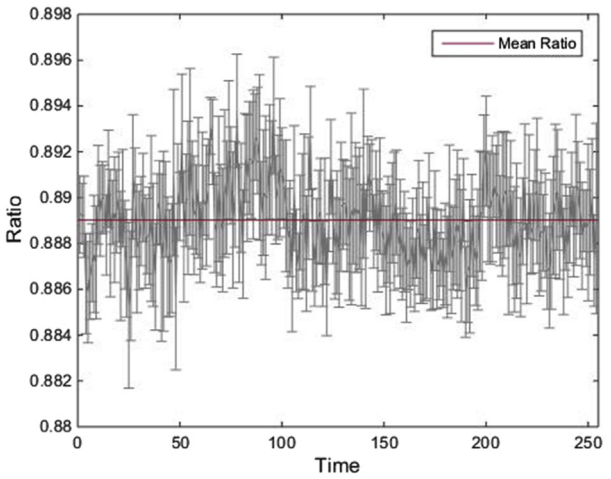

Fig. 8. Drift over 3 days with one measurement every 15 min in a sealed container, of artificial seawater, pH 8.1 salinity 35.

maintenance of another system coupled to the same underway seawater supply. Certified reference material was analysed at the halfway point of the run of each spot to correct for manufacturing offsets and drift as discussed above. The total drift of the spots measurements over the course of the cruise for both spots combined was 0.06 pH units before correction using the CRM measurement. This drift exceeds the error in the calculated pH (±0.0062) from the CRM values. The shipboard precision (0.0074 pH, n = 10) was comparable to ISFET sensors [27]. The underway observations by the sensor of surface ocean pH_{tot} across the Southern Ocean transect were in the range pH 7.90–8.39, which is a larger range to that reported by Bellerby (pH 8.04–8.28 *in situ*) [81]. These observations demonstrate the range of environments visited during our cruise, which included regions with high primary productivity and consequently enhanced CO_2 uptake and enhanced pH values (e.g. pH 8.3–8.4 north of South Georgia, ca. 52°N, 38°W, see Fig. 9). The enhanced chlorophyll-*a* concentrations encountered in the Southern Ocean (maximum observed ca. 11.2 μg L^1), may have resulted in a decrease in R, and in future on-line filtration prior to pH analysis should preferably be undertaken. The intense blooms are less common in other open ocean regions, due to a lack of macronutrients to support enhanced phytoplankton growth.

3.8. Current limitations and future directions

The pH spots provided continuous underway data in a challenging ocean region for which there is a lack on carbonate chemistry data. The day-to-day operation of the sensor was simple and trouble free. The precision of the spot in its current configuration is 0.0074 pH (n = 10), comparable to ISFET sensors but inferior to spectrophotometric pH systems. One limitation of the optode sensor is the observed drift in response over several weeks at sea. The precision and drift issues are likely caused by the low apparent pK_a' of the indicator (6.93 at 20 °C) in relation to the intended open ocean seawater range of pH 7.8–8.3, and the increased chlorophyll concentrations. To overcome these issues it is advisable to investigate alternative indicator dyes with more basic apparent pK_a' values and potentially greater stability. Schröder et al. [53] investigated two potential immobilised indicators, which were carboxyfluorescein derivatives, that showed similar temperature and salinity dependences to those observed in this study, but had pK_a' values (8.16 and 8.57) more suited to seawater measurements. Furthermore, the use of a spectrophotometric sensor in the calibration procedure will improve the precision on the reference pH measurements, and thereby moving the precision and accuracy of the optode closer to that of spectrophotometric systems. Efforts to develop improved pH spots for ocean measurements are currently undertaken in academic-industry collaborations as part of international research projects (e.g. SenseOcean and Atlantos, European Union Funded), and novel pH optodes will emerge over the coming years.

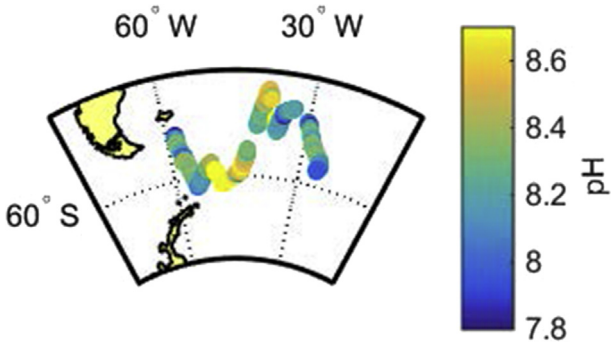

Fig. 9. Plot of underway pH determined with the optode sensor plotted along the cruise track.

Further developments with the optode presented herein should focus on the use of spectrophotometric system (instead of pH glass electrode) in calibrations to reduce the pH error in the optode algorithm, and more detailed investigations into the chlorophyll dependence of R, particularly at low chlorophyll concentrations. While more frequent use of CRM materials should be undertaken to correct for and remove drift in the system during deployment, application of an indicator with pK_a' values closer to average seawater pH (8.1) may largely eliminate this requirement.

In future, pH optode deployments (with the spot used in this study or others) should utilise a high performance temperature sensor alongside the optode to provide a more realistic determination of measurement temperature for the conversion from R to pH. In this study, we used filters, dichroic beam splitter and a PMT for the more specialised laboratory experiments and shipboard deployment, to investigate the effectiveness of the t-DLR technique and to employ low intensity excitation levels. However, for future *in situ* deployments, the use of a photodiode as a detection system and a reduced number of filters should be investigated in order to simplify the system and allow more widespread applications, as with the oxygen optodes.

4. Conclusion

This work has evaluated an optode pH sensor for measurement of ocean pH. We investigated temperature and salinity dependences, metrology and the longevity of a commercially available pH sensor spot across a pH range 7.6–8.2. The lifetime of the spot was improved with the use of low optical power for excitation and repeated short illumination times, while the response time of the spot was observed to be 50 s. The temperature dependence (−0.046 pH $°C^{-1}$ from 5 to 25 °C) and salinity dependence (−0.01 pH psu^{-1} over salinity 5–35) were accounted for using a calibration algorithm. This simplicity is an advantage compared to the individual calibrations required for ISFET and glass pH electrodes. The algorithm was tested through deployment as an underway sensor in the Southern Ocean, which displayed strong pH, chlorophyll and temperature gradients. A precision of 0.0074 pH was observed at sea, but the optode demonstrated drift of 0.06 pH over the period of the cruise (4 weeks), which was corrected for using CRM measurement. In a lab based experiment we found a drift of only 0.00014 R over 3 a day period (ca. 0.0004 pH, at 25 °C, salinity 35), suggesting that with further improvements to the deployment system drift may not be a significant issue. We suggest further investigation into alternative pH indicators with more suitable pK_a' values for surface ocean measurements, to improve the precision and limit any potential drift. With regular CRM calibrations, the spot characterised in this study is suitable for coastal deployments where pH precision requirements are lower. Optode technology is still in its infancy, and this study along with the now widespread use of oxygen optodes demonstrates the potential of this technology. Ongoing developments in spot technology will aim to deliver optode pH sensors over the coming years for oceanic deployments.

Acknowledgements

We are very grateful to Chris Daniels for culturing and providing the *E. Huxleyi* samples. We are also grateful to the NOCS sensors group, in particular Chris Cardwell and Iain Ogilvie for their help and advice with the hardware. A special thanks for the crew of the

R.R.S. *James Clark Ross* for their support during cruise JR274. The Analytical Chemistry Trust Fund, funded by the Royal Society for Chemistry and the Natural Environment Research Council (NE/I019638/1), supports this work. The Natural Environment Research Council as part of the UK Ocean Acidification Program NE/H017348/1 funded the R.R.S. *James Clark Ross* JR274 cruise.

We would also like to thank two anonymous reviewers for their constructive comments, which greatly improved this manuscript.

References

[1] P. Ciais, et al., Carbon and other biogeochemical cycles, in: T.F. Stocker, et al. (Eds.), Climate Change 2013: the Physical Science Basis. Contribution of Working Group 1 to the Fifth Assessment Report of the Intergovernmental Panel on Climate Change, Cambridge University Press, Cambridge, United Kingdom and New York, N.Y., U.S.A, 2013.
[2] J.G. Canadell, et al., Contributions to accelerating atmospheric CO_2 growth from economic activity, carbon intensity, and efficiency of natural sinks, Proc. Natl. Acad. Sci. U. S. A. 104 (47) (2007) 18866–18870.
[3] C. Le Quéré, et al., Trends in the sources and sinks of carbon dioxide, Nat. Geosci. 2 (2009) 831–836.
[4] N.L. Bindoff, et al., Observations: oceanic climate change and sea level, in: S. Solomon, et al. (Eds.), Contribution of Working Group I to the Fourth Assessment Report of the Intergovernmental Panel on Climate Change, Cambridge University Press, Cambridge, United Kingdom and New York, NY, USA, 2007, pp. 385–432.
[5] J.E. Dore, et al., Physical and biogeochemical modulation of ocean acidification in the central North Pacific, Proc. Natl. Acad. Sci. U. S. A. 106 (30) (2009) 12235–12240.
[6] R.H. Byrne, et al., Direct observations of basin-wide acidification of the North Pacific Ocean, Geophys. Res. Lett. 37 (2) (2010).
[7] M.Z. Jacobson, Studying ocean acidification with conservative, stable numerical schemes for nonequilibrium air-ocean exchange and ocean equilibrium chemistry, J. Geophys. Res. 110 (D7) (2005).
[8] IPCC, in: J.T. Houghton, et al. (Eds.), Climate Change 2001: the Scientific Basis. Contribution of Working Group I to the Third Assessment Report of the Intergovernmental Panel on Climate Change, Cambridge University Press, Cambridge, United Kingdom and New York, NY, USA, 2001, p. 881.
[9] K. Caldeira, M.W. Wickett, Ocean model predictions of chemistry changes from carbon dioxide emissions to the atmosphere and ocean, J. Geophys. Res. 110 (C9) (2005).
[10] C.L. Sabine, et al., The oceanic sink for anthropogenic CO_2, Science 305 (2004) 367–371.
[11] N. Bednaršek, et al., Extensive dissolution of live pteropods in the Southern Ocean, Nat. Geosci. 5 (2012) 881–885.
[12] O.S. Wolfbeis, Chemical sensing using indicator dyes, in: J. Dakin, B. Culshaw (Eds.), Optical Fiber Sensors, Artech House, Boston-London, 1997, pp. 53–107.
[13] A. Körtzinger, J. Schimanski, High quality oxygen measurements from profiling floats: a promising new technique, J. Atmos. Ocean. Technol. 22 (2004).
[14] M. Larsen, et al., A simple and inexpensive high resolution color ratiometric planar optode imaging approach: application to oxygen and pH sensing, Limnol. Oceanogr. Methods 9 (2011) 348–360.
[15] V.M.C. Rérolle, et al., Seawater-pH measurements for ocean-acidification observations, TrAC Trends Anal. Chem. 40 (2012) 146–157.
[16] A.G. Dickson, The measurement of sea water pH, Mar. Chem. 44 (2–4) (1993) 131–142.
[17] R.H. Byrne, et al., Seawater pH measurements: an at-sea comparison of spectrophotometric and potentiometric methods, Deep Sea Res. Part I Oceanogr. Res. Pap. 35 (8) (1988) 1405–1410.
[18] Idronaut, Cylindrical, High Pressure Glass Membrane pH Electrode, 1995 [cited 2014 13/11/2014]; Available from: http://www.idronaut.it/products-ph-sensors-water-quality.
[19] R. Kadis, I. Leito, Evaluation of the residual liquid junction potential contribution to the uncertainty in pH measurement: a case study on low ionic strength natural waters, Anal. Chim. Acta 664 (2) (2010) 129–135.
[20] R.A. Easley, R.H. Byrne, Spectrophotometric calibration of pH electrodes in seawater using purified m-Cresol purple, Environ. Sci. Technol. 46 (9) (2012) 5018–5024.
[21] C.-y. Tan, et al., A long-term in situ calibration system for chemistry analysis of seawater, J. Zhejiang Univ. Sci. A 11 (9) (2010) 701–708.
[22] A.V. Borges, M. Frankignoulle, Daily and seasonal variations of the partial pressure of CO_2 in surface seawater along Belgian and southern Dutch coastal areas, J. Mar. Syst. 19 (1999) 251–266.
[23] M. Frankignoulle, A.V. Borges, Direct and indirect pCO_2 measurements in a wide range of pCO_2 and salinity values (The Scheldt Estuary), Aquat. Geochem. 7 (2001) 267–273.
[24] N. Le Bris, P.-M. Sarradin, S. Pennec, A new deep-sea probe for in situ pH measurement in the environment of hydrothermal vent biological communities, Deep Sea Res. Part I Oceanogr. Res. Pap. 48 (8) (2001) 1941–1951.
[25] T.R. Martz, J.G. Connery, K.S. Johnson, Testing the honeywell durafet for seawater pH applications, Limnol. Oceanogr. Methods 8 (2010) 172–184.
[26] Satlantic. SeaFET™ Ocean pH Sensor, 2014 [cited 2014 13/11/2014]; Available from: http://satlantic.com/seafet.
[27] N. Le Bris, D. Birot, Automated pH-ISFET measurements under hydrostatic pressure for marine monitoring application, Anal. Chim. Acta 356 (1997) 205–215.
[28] V.K. Khanna, Remedial and adaptive solutions of ISFET non-ideal behaviour, Sens. Rev. 33 (3) (2013) 228–237.
[29] P.J. Bresnahan, et al., Best practices for autonomous measurement of seawater pH with the honeywell durafet, Methods Oceanogr. 9 (2014) 44–60.
[30] T.R. Martz, et al., A submersible autonomous sensor for spectrophotometric pH measurements of natural waters, Anal. Chem. 75 (8) (2003) 1844–1850.
[31] V.M.C. Rérolle, et al., Development of a colorimetric microfluidic pH sensor for autonomous seawater measurements, Anal. Chim. Acta 786 (5) (2013) 124–131.
[32] S. Aßmann, C. Frank, A. Körtzinger, Spectrophotometric high-precision seawater pH determination for use in underway measuring systems, Ocean Sci. 7 (5) (2011) 597–607.
[33] M.P. Seidel, M.D. DeGrandpre, A.G. Dickson, A sensor for in situ indicator-based measurements of seawater pH, Mar. Chem. 109 (2008) 18–28.
[34] Y. Nakano, et al., Simultaneous vertical measurements of in situ pH and CO_2 in the sea using spectrophotometric profilers, J. Oceanogr. 62 (2006) 71–81.
[35] X. Liu, et al., Spectrophotometric measurements of pH in-situ: laboratory and field evaluations of instrumental performance, Environ. Sci. Technol. 40 (16) (2006) 5036–5044.
[36] K. Friis, A. Körtzinger, D.W.R. Wallace, Spectrophotometric pH measurement in the ocean: requirements, design, and testing of an autonomous charge-coupled device detector system, Limnol. Oceanogr. Methods 2 (2004) 126–136.
[37] R.G.J. Bellerby, et al., A high precision spectrophotometric method for on-line shipboard seawater pH measurements: the automated marine pH sensor (AMpS), Talanta 56 (1) (2002) 61–69.
[38] Z.A. Wang, et al., In situ sensor technology for simultaneous spectrophotometric measurements of seawater total dissolved inorganic carbon and pH, Environ. Sci. Technol. 49 (7) (2015) 4441–4449.
[39] M.D. DeGrandpre, et al., In situ measurements of seawater pCO_2, Limnol. Oceanogr. 40 (5) (1995) 969–975.
[40] K.E. Harris, M.D. DeGrandpre, B. Hales, Aragonite saturation state dynamics in a coastal upwelling zone, Geophys. Res. Lett. 40 (11) (2013) 2720–2725.
[41] D. Wencel, T. Abel, C. McDonagh, Optical chemical pH sensors, Anal. Chem. 86 (1) (2014) 15–29.
[42] C. Boniello, et al., Dual-lifetime referencing (DLR): a powerful method for on-line measurements of internal pH in carrier-bound immobilized biocatalysts, BMC Biotechnol. 12 (11) (2012).
[43] Y. Tian, et al., A fluorescent colorimetric pH sensor and the influences of matrices on sensing performances, Sensors Actuators B Chem. 188 (2013) 1–10.
[44] A. Hakonen, S. Hulth, A high-precision ratiometric fluorosensor for pH: Implementing time-dependent non-linear calibration protocols for drift compensation, Anal. Chim. Acta 606 (1) (2008) 63–71.
[45] M.I. Stich, L.H. Fischer, O.S. Wolfbeis, Multiple fluorescent chemical sensing and imaging, Chem. Soc. Rev. 39 (8) (2010) 3102–3114.
[46] I. Klimant, et al., Dual Lifetime Referencing (DLR) – a new scheme for converting fluorescence intensity into a frequency-domain or time-domain information, in: B. Valeur, J.-c. Brochon (Eds.), New Trends in Fluorescence Spectroscopy: applications to Chemical and Life Science, Springer-Verlag, Germany, 2001, pp. 257–274.
[47] H. Szmacinski, J.R. Lakowicz, Lifetime-based sensing, in: J. Lakowicz (Ed.), Topics in Fluorescence Spectroscopy Volume 4: Probe Design and Chemical SensingKluwer Academic Publishers, New York, 1994, pp. 295–329.
[48] G. Liebsch, et al., Fluorescent imaging of pH with optical sensors using time domain dual lifetime referencing, Anal. Chem. 73 (17) (2001) 4354–4363.
[49] G. Liebsch, et al., Luminescence lifetime imaging of oxygen, ph and carbon dioxide distribution using optical sensors, Appl. Spectrosc. 54 (4) (2000) 548–559.
[50] T.D. Bradrick, J.E. Churchich, Time-resolved fluorescence and phosphorescence spectroscopy, in: M.G. Gore (Ed.), Spectrophotometry and Spectrofluorimetry, Oxford University Press, Great Clarendon Street, Oxford, 2000, pp. 69–97.
[51] A. Hakonen, S. Hulth, A high-performance fluorosensor for pH measurements between 6 and 9, Talanta 80 (5) (2010) 1964–1969.
[52] V.M.C. Rérolle, et al., Seawater-pH measurements for ocean-acidification observations, Trac Trends Anal. Chem. 40 (2012) 146–157.
[53] C. Schröder, B.M. Weidgans, I. Klimant, pH fluorosensors for use in marine systems, Analyst 130 (6) (2005) 907–916.
[54] Q. Zhu, R.C. Aller, Y. Fan, High-performance planar pH fluorosensor for two dimensional pH measurements in marine sediment and water, Environ. Sci. Technol. 39 (2005) 8906–8911.
[55] H. Stahl, et al., Time-resolved pH imaging in marine sediments with a luminescent planar optode, Limnol. Oceanogr. Methods 4 (2006) 336–345.
[56] D. Wencel, B.D. MacCraith, C. McDonagh, High performance optical ratiometric sol–gel-based pH sensor, Sensors Actuators B Chem. 139 (1) (2009) 208–213.
[57] J.J. Barron, C. Ashton, L. Geary, The effects of temperature on pH measurement, in: 57th Annual Meeting of the International Society of Electrochemistry,

Edinburgh, Technical Services Department, Reagecon Diagnostics Ltd, Ireland, 2006.
[58] H.N. Zhang, R.H. Byrne, Spectrophotometric pH measurements of surface seawater at in-situ conditions: absorbance and protonation behavior of thymol blue, Mar. Chem. 52 (1) (1996) 17–25.
[59] K.W. Pratt, Measurement of pHT values of tris buffers in artificial seawater at varying mole ratios of tris:tris·HCl, Mar. Chem. 162 (2014) 89–95.
[60] A.I. Vogel, in: G.H. Jeffery, et al. (Eds.), Vogel's Textbook of Quantitative Chemical Analysis, fifth ed., Longman Scientific & Technical, Essex, England, 1989.
[61] M.G. Mellon, V.N. Morris, Standardizing acids and bases with borax, Ind. Eng. Chem. 17 (2) (1925) 145–146.
[62] Sigma–Aldrich, Trizma base Product Information. Sigma Aldrich: Sigma-aldrich.com.
[63] B. Valeur, Molecular Fluorescence: Principles and Applications, WILEY-VCH, Germany, 2002.
[64] S. Derinkuyu, et al., Fiber optic pH sensing with long wavelength excitable Schiff bases in the pH range of 7.0–12.0, Anal. Chim. Acta 588 (1) (2007) 42–49.
[65] H.M. Goncalves, et al., Fiber optic lifetime pH sensing based on ruthenium(II) complexes with dicarboxybipyridine, Anal. Chim. Acta 626 (1) (2008) 62–70.
[66] L.E.V. Salgado, C. Vargas-Hernández, Spectrophotometric determination of the pKa, isosbestic point and equation of absorbance vs. pH for a universal pH indicator, Am. J. Anal. Chem. 05 (17) (2014) 1290–1301.
[67] A. Tengberg, et al., Evaluation of a lifetime-based optode to measure oxygen in aquatic systems, Limnol. Oceanogr. Methods 4 (2006) 7–17.
[68] A.G. Dickson, C.L. Sabine, J.R. Christian, in: A.G. Dickson, C.L. Sabine, J.R. Christian (Eds.), Guide to Best Practices for Ocean CO_2 Measurements, PICES Special Publication, 2007.
[69] D. Pierrot, E. Lewis, D.W.R. Wallace, MS Excel Program Developed for CO_2 System Calculations, Carbon Dioxide Information Analysis Center,Oak Ridge National Laboratory, U.S. Department of Energy, Oak Ridge, Tennessee, 2006.
[70] R.S. Roy, et al., The dissociation constants of carbonic acid in seawater at salinities 5 to 45 and temperatures 0 to 45°C, Mar. Chem. 44 (1993) 249–267.
[71] A.G. Dickson, Standard potential of the reaction $AgCl(s) + 1/2H_2(g) = Ag(s) + HCl(aq)$ and the standard acidity constant of the bisulfate ion in synthetic seawater from 273.15 K to 318.15 K, J. Chem. Thermodyn. 22 (2) (1990) 113–127.
[72] K. Lee, et al., The universal ratio of boron to chlorinity for the North Pacific and North Atlantic oceans, Geochim. Cosmochim. Acta 74 (6) (2010) 1801–1811.
[73] S. Capel-Cuevas, et al., Full-range optical pH sensor based on imaging techniques, Anal. Chim. Acta 681 (1–2) (2010) 71–81.
[74] S. Hulth, et al., A pH plate fluorosensor (optode) for early diagenetic studies of marine sediments, Limnol. Oceanogr. 47 (1) (2002) 212–220.
[75] W. Stumm, J.J. Morgan, Aquatic Chemistry: Chemical Equilibria and Rates in Natural Water, in: Environmental Science and Technology, Wiley-Interscience, Canada, 1996, p. 1040.
[76] P. Atkins, J. de Paula, Physical Chemistry, W. H. Freeman, 2006.
[77] G.F. Kirkbright, R. Narayanaswamy, N.A. Welti, Fibre-optic pH probe based on the use of an immobilised colorimetric indicator, Analyst 109 (1984) 1025–1028.
[78] A. Hakonen, et al., A potential tool for high-resolution monitoring of ocean acidification, Anal. Chim. Acta 786 (2013) 1–7.
[79] J. Janata, Do optical sensors really measure pH? Anal. Chem. 59 (9) (1987) 1351–1356.
[80] B. Yang, et al., Seawater pH measurements in the field: a DIY photometer with 0.01 unit pH accuracy, Mar. Chem. 160 (0) (2014) 75–81.
[81] R.G.J. Bellerby, D.R. Turner, J.E. Robertson, Surface pH and pCO_2 distributions in the Bellinghausen Sea, Southern Ocean, during the early Austral Summer, Deep Sea Res. II 42 (4–5) (1995) 1093–1107.